Results in Chemistry 17 (2025) 102603

Contents lists available at ScienceDirect

Results in Chemistry

journal homepage: www.sciencedirect.com/journal/results-in-chemistry

Enhanced adsorption of ciprofloxacin by biochar with acid and alkali modification: Performance comparison and mechanism analysis

Hui Wang [a,b,*], Haoliang Wang [d], Siyamak Shahab [b,c,*], Hezhang Cheng [b,*], Mikhail Atroshko [b], Xianpeng Wang [e], Meng Ye [b,*]

[a] School of Health Science and Nursing, Shanghai Sipo Polytechnic,1408 Chengnan Road, Shanghai 201399, China
[b] International Sakharov Environmental Institute, Belarusian State University, 23/1 Dolgobrodskaya str., Minsk 220070, Republic of Belarus
[c] Institute of Physical Organic Chemistry, National Academy of Sciences of Belarus, 13 Surganov Str., Minsk 220072, Byelorussia
[d] College of Marine Technology and Environment, Dalian Ocean University, Dalian 116023, China
[e] International Institute of Management and Entrepreneurship, Slavinskogo street, Minsk 220086, Republic of Belarus

ARTICLE INFO

Keywords:
Biochar
Acid-alkali modification
Ciprofloxacin adsorption
-COOH active site
Pore structure-activity relationship
DFT mechanism analysis

ABSTRACT

The widespread presence of antibiotic residues in aquatic environments, resulting from the extensive use of antibiotics in livestock and aquaculture, has driven the search for effective remediation methods. Adsorption, particularly using biochar, has emerged as a promising approach. In this study, rice straw-derived biochar (denoted as B5) modified with phosphoric acid (H_3PO_4-modified B5, PB5) and potassium hydroxide (KOH-modified B5, KB5) at the same concentration was investigated for ciprofloxacin (CIP) adsorption. PB5 exhibited a maximum Langmuir adsorption capacity of 25.6 mg/g for CIP, surpassing KOH-modified (8.77 mg/g) and unmodified biochar (3.71 mg/g). The optimized pH for adsorption was 3.0–7.0, where electrostatic interactions and hydrogen bonding dominated. Characterization revealed that acid-base modification altered the surface morphology, pore structure, and functional groups of biochar. PB5 exhibited a rougher surface, increased porosity, and enhanced oxygen-containing functional groups, while KB5 had a more pronounced increase in large specific surface area (SSA). Adsorption experiments indicated a multistage process involving chemisorption, external diffusion, and intraparticle diffusion. The pseudo-second-order model and the Freundlich isotherm best described the adsorption behavior, indicating chemisorption-dominated non-homogeneous adsorption. Density Functional Theory (DFT) calculations and X-ray photoelectron spectroscopy (XPS) analysis identified the -COOH group on biochar as the main active site for CIP adsorption, with a strong dual-force interaction. pH and anion studies showed that pH affected adsorption via electrostatic interactions, and divalent anions, especially SO_4^{2-}, inhibited adsorption, more so for PB5 due to its larger pore size. This study elucidates the distinct adsorption mechanisms of acid and alkali-modified biochar for CIP, providing valuable insights for the design and optimization of biochar for antibiotic removal in water treatment, Further research should explore diverse antibiotic models and advanced research tools to address real-world environmental challenges.

1. Introduction

Antibiotics play an important role in disease prevention and the protection of animals against disease. They are commonly used in livestock and aquaculture [1,2]. It is worth noting that antibiotics ingested by organisms are difficult to fully utilize. More than 30–90 % of antibiotics are incompletely metabolized in organisms, resulting in the inevitable discharge of antibiotics and their metabolites into the aquatic environment [3,4]. In addition, due to the chemical stability of antibiotics and the fact that they are not easily broken down. Antibiotics are frequently detected in various natural water sources, such as surface water, groundwater, and even drinking water [5,6], where the concentration of antibiotics ranges from 0.0005 to 56,000 μg/L [7]. Most importantly, aquatic environments that contain large quantities of antibiotic residues can cause serious environmental problems [8]. They can have serious negative impacts on freshwater animals and plants, including non-target organisms such as algae, microorganisms, macrophytes, zooplankton, and fish. They may accumulate in top predators

* Corresponding authors at: International Sakharov Environmental Institute, Belarusian State University, 23/1 Dolgobrodskaya str., Minsk 220070, Repubilc of Belarus.
E-mail addresses: wanghui@iseu.by (H. Wang), kbb@iseu.by (S. Shahab), cheng_hezhang@iseu.by (H. Cheng), yemeng@sipo.sicfl.edu.cn (M. Ye).

https://doi.org/10.1016/j.rechem.2025.102603
Received 23 April 2025; Accepted 7 August 2025
Available online 8 August 2025

and plants through the food chains, posing a potential threat to human health [9]. Moreover, the accumulation of antibiotics in the environment promotes the development of antibiotic-resistant bacteria (ARBs) and accelerates the spread of antibiotic-resistant genes (ARGs) among various bacterial strains [3,10]. This phenomenon can lead to the emergence of highly resilient pathogens and disrupt the balance of the microbial ecosystem [11,12]. Therefore, reducing antibiotic residues in water bodies will effectively curb the hazards and risks associated with the spread of ARGs and reduce the serious threat they pose to human health [13].

Adsorption is a cost-effective, scalable, and energy-efficient method for antibiotic removal, avoiding secondary pollution from chemical treatments. Unlike advanced oxidation processes, adsorption preserves the structural integrity of antibiotics and minimizes toxic byproducts [14]. In this regard, researchers have developed various adsorbents for antibiotic removal, including carbon-based materials, polymers, and other natural/synthetic materials [15]. Among them, the use of biochar made from biomass waste has attracted much attention by showing various advantages such as low cost, high availability, easy modification, environmentally friendly, reusable, and efficient pollutant remediation potential [16–18]. In particular, the use of biochar in wastewater treatment is a promising solution because biochar has a number of structural properties, including a large specific surface area (SSA), a high pore structure, and a wide variety of surface functional groups, which make its adsorption capacity extremely strong and highly modifiable [19]. Therefore, biochar has become a widely used material for environmental remediation. Due to the limited porosity and functional groups of biochar and the difficulty of recycling, to break through the adsorption bottleneck of the structural properties of biochar, researchers investigated the effects of the raw materials, pyrolysis temperature, and production process on the adsorption performance of biochar, and obtained sufficient reference data on the structure and performance [20,21]. However, modifying the physical preparation conditions of biochar was insufficient to enhanced adsorption performance, and thus researchers have proposed several chemical modification methods.

Several common modification methods have been proposed to enhance the adsorption characteristics of biochar, including acid-base modification, metal modification, and other techniques [22–24]. Compared with metal modification, acid-base modification is simpler, less costly, and does not lead to secondary pollution. Acid-base modification primarily alters the SSA and pore structure as well as functional groups of biochar [25].

Acid modification removes impurities such as minerals from biochar and introduces acidic groups (e.g., carboxyl and amine groups) to the surface, which play a crucial role in enhancing in increasing the adsorption performance of biochar [26]. Alkaline modification, typically using sodium hydroxide (NaOH) and potassium hydroxide solutions (KOH), enhances the oxygen functional groups in biochar while dissolving ash and coagulating organic matter [27]. Although the enhancement of adsorption of organic pollutants by acid- or base-modified biochar has been reported in related studies, the extent to which the type and concentration of the acid or base affect the modification of biochar is unknown. Therefore, it is necessary to investigate the changes in the structural properties of biochar under the same concentration of acid and alkali, and the structure-activity relationship of acid and alkali modification on the adsorption of organic pollutants by biochar.

To address this knowledge gap, we chose CIP as a model compound, which is a third-generation fluoroquinolone antibiotic widely used in veterinary medicine and the human body because of its high clinical efficacy and antimicrobial activity [28,29]. This study addresses the knowledge gap in understanding how acid-base modifications under identical concentrations affect biochar's structural properties and adsorption mechanisms for antibiotics. Unlike previous studies focusing on single modification methods or varying concentrations, we systematically compare phosphoric acid (H_3PO_4) and potassium hydroxide (KOH) modifications at the same molarity (1.0 mM) to elucidate their distinct impacts on biochar's pore structure, functional groups, and adsorption performance. Novelty lies in the integration of advanced characterization techniques—including scanning electron microscopy (SEM), X-ray photoelectron spectroscopy (XPS), Fourier-transform infrared spectroscopy (FTIR), and Brunauer-Emmett-Teller (BET) analysis—with density functional theory (DFT) calculations. This approach identifies the role of carboxyl (-COOH) groups as primary adsorption sites. Our approach provides a clear structure-activity relationship, demonstrating that acid modification enhances oxygenated functional groups, while alkali modification primarily increases surface area. These findings offer practical insights for designing biochar tailored to the removal of specific antibiotics in water treatment applications.

2. Materials and methods

2.1. Chemicals and reagents

The antibiotic standard (Ciprofloxacin, CIP) was purchased from Sigma-Aldrich. All other chemicals including KOH, H_3PO_4, and H_2SO_4, were obtained from Aladdin, China. All chemicals and reagents were analytical grade and used without further purification.

2.2. Biochar preparation

Rice straw was collected from the agricultural fields in Yiliang County, Kunming, China. The collected straw (elemental composition: C 38.6 %, O 43.2 %, N 0.6 %, S 0.4 %, H 5.2 %) was washed, dried, chopped, and pulverized to particles <2 mm in size for use as raw material. Pyrolysis was conducted in a tube furnace under N_2 atmosphere at 500 °C for 4 h to produce biochar (denoted as B5). The resulting biochar was ground, sieved (100 mesh), and stored in airtight containers. The acid/alkali-modified biochar was prepared as follows. 3.0 g of B5 was dispersed in phosphoric acid solution (95.0 %, 1.0 mM, 100.0 mL) and potassium hydroxide (KOH) solution (>99.0 %, 1.0 mM, 100.0 mL) with continuous stirring for 12 h. The reacted biochar suspension was filtered to obtain solid biochar pellets, and then the biochar pellet samples were washed repeatedly with ultrapure water and dried at 60 °C to remove moisture. The phosphoric acid-modified biochar was labeled as PB5, and the KOH-modified biochar was named KB5.

2.3. Characterization of biochar

The types and relative content of surface functional groups were characterized using FTIR (Varian 640-IR, USA) and XPS (ESCALAB 250 Xi, Thermo Fisher Scientific, USA). The morphology of biochar was evaluated using SEM (ZEISS SUPRA 40, Germany). The SSA and pore structure of biochar were characterized using N_2 adsorption and desorption (ASAP 2020, USA). The zeta potential of biochar was determined by Malvern (Nano ZS90, ZEN350, UK). The detailed experiment parameters are provided in the Supporting Information Text S1.

2.4. Adsorption experiments

Batch adsorption experiments were conducted in 40.0 mL brown vials containing 15.0 mg of biochar and 10.0 mL of CIP stock solution at different concentrations. For kinetic studies, aliquots were collected at 0.5, 1, 2, 4, 8, 12, and 18 h for adsorption kinetics experiments. For adsorption equilibrium, all samples were stirred in a thermostatic shaking incubator at 150 rpm for 18 h. To establish adsorption isotherms, CIP solutions were prepared at different concentrations (2, 4, 6, 10, and 15 $mg \bullet L^{-1}$). The effect of pH on CIP adsorption was investigated by adding a certain amount of adsorbent to the initial CIP solutions at pH 3.0, 7.0, and 9.0. The pH was varied using KOH (5.0×10^{-2} M) or H_2SO_4 (5×10^{-2} M). The effect of different anions on the CIP adsorption

performance of biochar was investigated at the same molar concentration. After adsorption, 1.0 mL of supernatant was withdrawn using a syringe and filtered through a 0.45 μm PVDF disk filter, and the filtrate was collected and used to determine the residual CIP concentration. The CIP concentration was detected using UV–vis spectrophotometry at 270.0 nm. All experiments performed in triplicate.

2.5. Data processing and DFT calculations

The amount of antibiotic adsorbed by biochar (Q_e, mg/g) was calculated from the concentration difference between the initial solution (C_0, mg/L) and the equilibrium solution (C_e, mg/L). The adsorption kinetics are simulated with pseudo-first-order, pseudo-second-order [30], Elovich [31], and intra-particle diffusion Eqs. [32], respectively. The adsorption kinetics are simulated with the Langmuir isotherm model [33], the Freundlich isotherm model [34], Temkin model [35], respectively. The details of data processing are described in Supporting Information Text S2.

The adsorption energy (E_{ad}) of CIP on biochar was calculated based on DFT calculations by using the Gaussian 09 software package [36,37]. The details of the calculation are described in Supporting Information Text S3.

3. Results and discussion

3.1. Characterization of biochar

The surface morphology and pore structure characteristics of B5, PB5, and KB5 were investigated using SEM. The surface of unmodified B5 particles was smooth, with a relatively regular pore structure that was in shape (Fig. S1). In contrast, PB5 and KB5 showed rough surfaces, higher porosity, and particle inhomogeneity, suggesting that acid-base modification altered the biochar's structural morphology. The irregular porous structure likely resulted from chemical reactions between the biochar surface and H_3PO_4/KOH, producing water vapor and carbon dioxide [38]. BET analysis measured the SSA, porosity, and pore size distribution of B5, PB5, and KB5. The N_2 adsorption-desorption isotherms and pore size distribution curves of the biochar are shown in Fig. 1a and Fig. 1b. By observing the N_2 adsorption behavior in this specific P/P_0 range, we could infer the changes in mesopore volume, pore size distribution, and surface area. The N_2 adsorption of PB5 and KB5 was mainly distributed in the range of 0.25 to 0.80 in the P/P_0 value, suggesting that the removal of tarry residues in the pristine biochar using H_3PO_4 and KOH improved the mesopore structure and maintain the porosity. The pore size distribution curves showed a mesoporous structure (2.0–50.0 nm) after acid-base modification, and the peaks of the pore size distributions of both PB5 and KB5 were located at 39 Å. KB5 showed a more pronounced enhancement of the pore volume

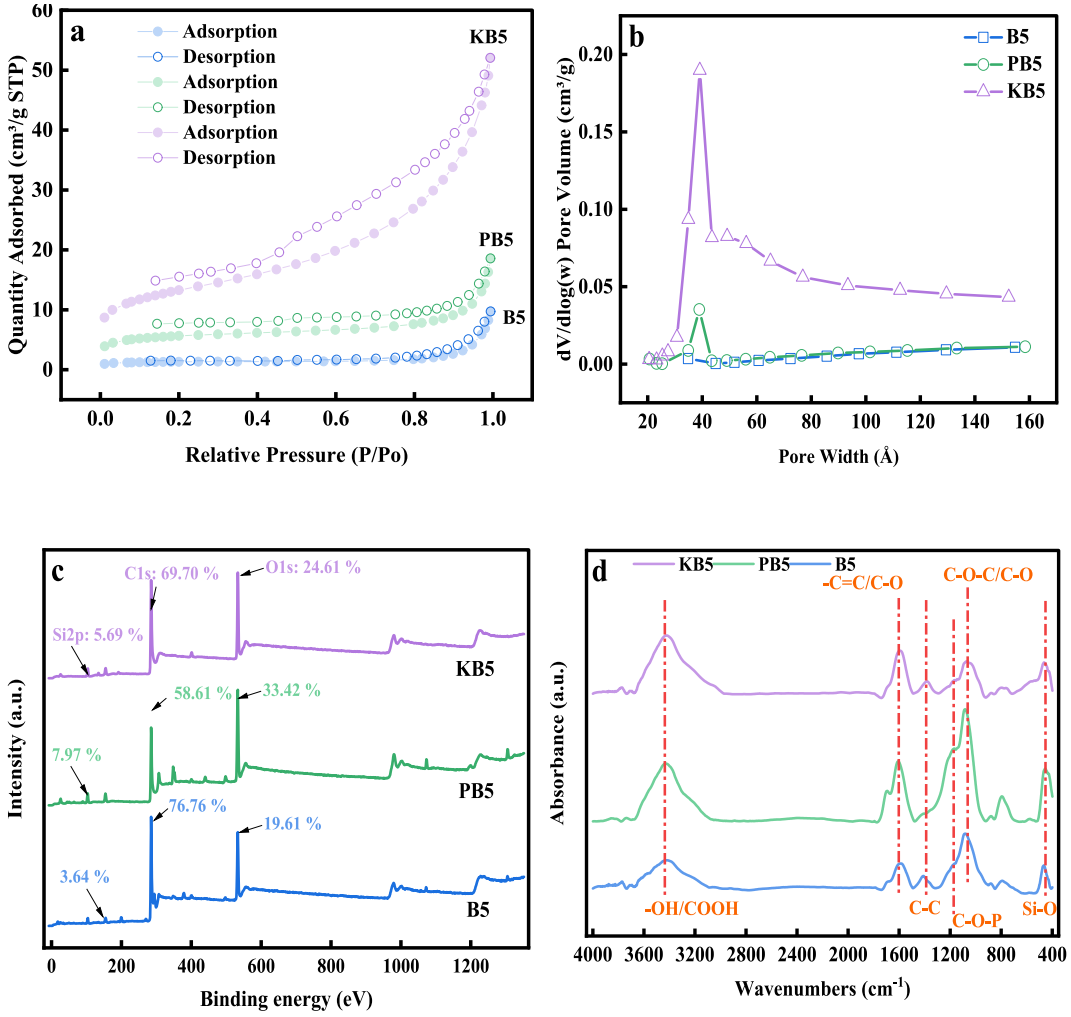

Fig. 1. (a) Adsorption and desorption curves of B5, PB5, and KB5 via BET analysis; (b)The pore size distribution curves of B5, PB5, and KB5; (c) The relative content of C, O, and Si by XPS spectra; (d) The functional groups of B5, PB5, and KB5 by FTIR spectra.

than PB5, indicating that KOH modification was more effective in modulating the pore structure of the biochar. The SSA of B5, PB5, and KB5 were 0.77, 1.86, and 5.92 m^2/g, respectively. H_3PO_4 and KOH modification increased the SSA by 2.4 and 7.7 times, and the total pore volume by 6.0 and 13.0 times, respectively. The average pore size of PB5 increased from 78.4 Å (B5) to 131.0 Å, and KB5 from 78.4 Å to 90.8 Å. Thus, the biochar activated by H_3PO_4 and KOH showed significant improvement in SSA, pore volume, and pore size, which may enhance the adsorption efficiency of biochar.

Given the high Si content in rice straw [39], XPS analysis revealed contents of C, XPS analysis revealed decreased C but increased Si content on the biochar surface after H_3PO_4/KOH treatment (Fig. 1c). This suggests ash removal exposed oxygenated functional groups. FTIR spectra further identified these groups (Fig. 1d): the characteristic peak (3432.0 cm^{-1}) of -OH/-COOH groups [40] was observed and its significant enhancement after modification may favor the absorption of pollutants. In addition, the stretching vibration peaks of C═C and C—O [41,42] in the aryl ring were around 1600.0 cm^{-1}, which were slightly elevated after modification by H_3PO_4 and KOH. In addition, the presence of a C—C aromatic ring at 1400.0 cm^{-1} further confirmed the structure of the aromatic ring, the peaks at 1100.0 cm^{-1} attachment were designated as C-O-C and C—O vibrational peaks [43], and the peaks located near 466.0 cm^{-1} were induced by Si—O vibration of inorganic SiO_2 [44]. Therefore, the larger change in functional groups on the surface of the biochar after H_3PO_4 and KOH treatments was the -OH/-COOH groups. Additionally, PB5's peak at 1170.0 cm^{-1} was attributed to C-O-P formation through H_3PO_4 dehydration on PB5 [45].

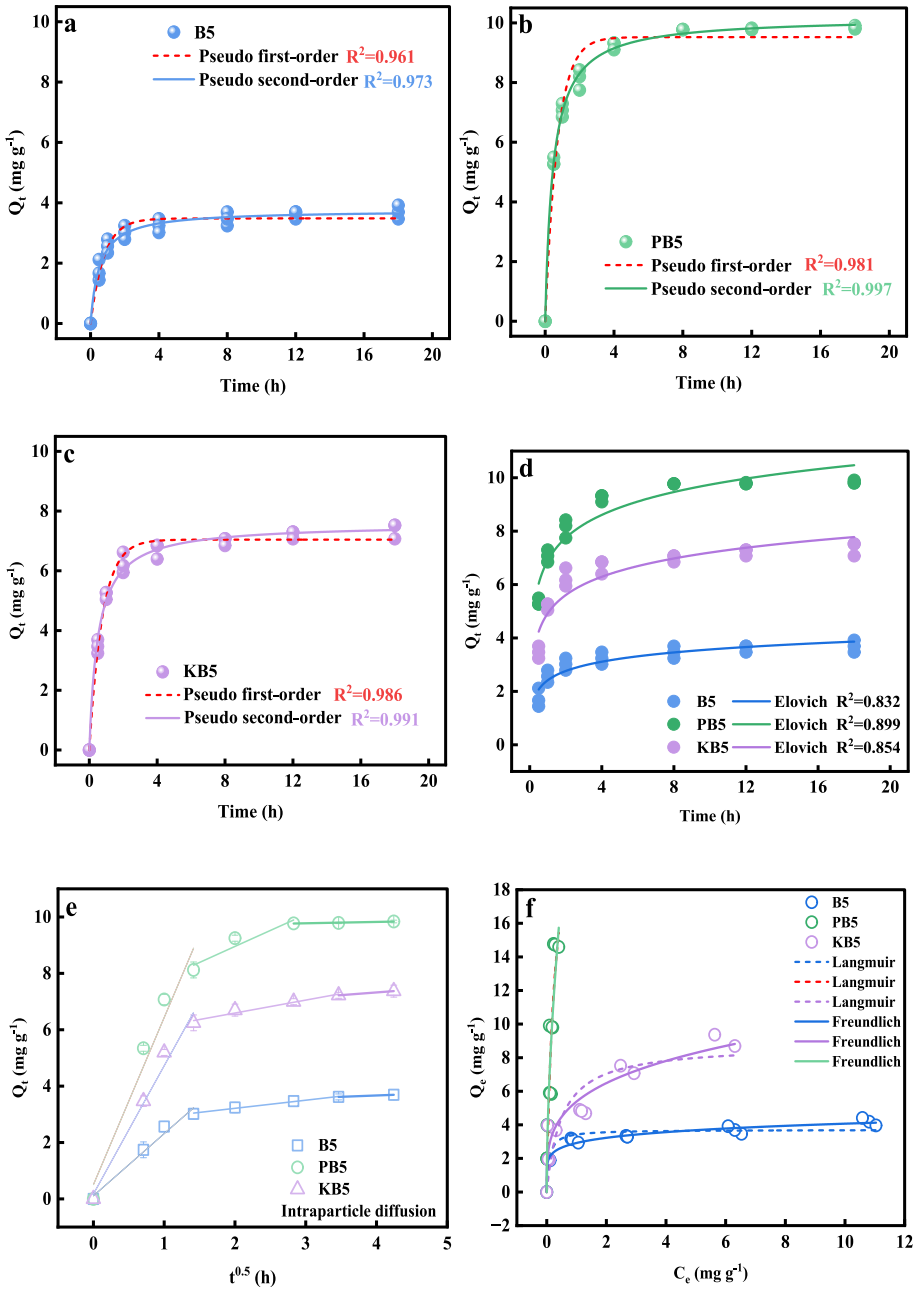

Fig. 2. (a, b, and c) The adsorption kinetics and models fitting of CIP by B5, PB5 and KB5 systems; (d) The Elovich kinetic model of CIP by B5, PB5 and KB5 systems; (e) The intraparticle diffusion model of CIP by B5, PB5 and KB5 systems; (f) Langmuir and Freundlich model fitting of isothermal experiments by B5, PB5 and KB5 systems.

3.2. Adsorption kinetics and isotherms

3.2.1. Kinetics

The adsorption kinetics of CIP on B5, PB5, and KB5 were investigated at an initial concentration of 10 mg/L (pH 7.0) over 18 h. The adsorbed CIP concentration (Q_t) at different time intervals is shown in Fig. 2a-c. During the initial stage, Q_t increased rapidly with time and reached equilibrium within 8 h. The Q_t values for PB5 and KB5 were significantly higher than those for B5, demonstrating that H_3PO_4 and KOH treatments enhanced adsorption efficiency. Notably, H_3PO_4 modification showed more pronounced improvement, suggesting acid modification as the preferred approach for biochar optimization.

experimentally investigated with an initial antibiotic concentration of 10 mg/L (pH 7.0) and a reaction period of 18 h. The solid phase concentration (Q_t) of CIP adsorbed on biochar at different times is shown in Fig. 2a-c. In the initial stage, *Q*t increased rapidly with the adsorption reaction time and reached equilibrium at 8 h around which equilibrium was reached. The adsorption Q_t values of CIP on PB5 and KB5 were higher compared to B5, which indicated that the H_3PO_4 and KOH treatments increased the adsorption efficiency of biochar. And the adsorption promotion was more significant after H_3PO_4 modification. Therefore, we believe that acid modification can be preferred when modulating biochar adsorption.

The adsorption mechanism was determined by fitting the experimental data using the pseudo-first-order kinetic (PFO) model, the pseudo-second-order kinetic (PSO) model, the Elovich kinetic model, and the intraparticle diffusion kinetic model [46,47]. The kinetic fitting curves for the CIP were shown in Fig. 2(a-d), and the derived parameters were summarized in Table S1. The PSO model has higher accuracy compared to the PFO model. The Elovich kinetic model exhibited relatively low R^2 values. These results suggested that the PSO model better described the adsorption mechanism of CIP on B5, PB5, and KB5. The chemisorption process, which was the limiting step for CIP removal, which involved chemical bonding between functional groups on the surface of biochar and CIP.

In addition, to further understand the adsorption kinetics, the experimental data were fitted using an intraparticle diffusion model. A linear plot of Q_t versus $t^{0.5}$ was presented in Fig. 2e, and the fitting results showed three linear components, which suggested that the adsorption process was multistage, and the adsorption reaction system could contain three processes: diffusion, adsorption, and equilibrium. The values of the intra-particle diffusion rate constants k_{i1} were significantly larger than k_{i2} and k_{i3} for the three reaction systems, indicating that diffusion of CIP molecules to the biochar surface dominated in the initial stage. Subsequently, adsorption and equilibrium processes occurred. Importantly, in this study, k_{i1}, $k_{i2,}$ and k_{i3} of CIP in PB5 were greater than those of B5 and KB5, suggesting that PB5 possessed a stronger mass driving force and more adsorption sites for CIP. In addition, C-value served as an index denoting the thickness of the boundary layer and could be employed to assess the diffusion resistance [48]. The C-values of all three biochar samples were C1 < C2 < C3 (all >0). The lower C values indicated that the initial liquid-phase diffusion resistance was lower, while the later diffusion resistance increased as the active sites were blocked by the adsorbent.

The above results indicate that the adsorption mechanism of CIP on B5, PB5 and KB5 was controlled by multiple mechanisms, including chemisorption, external diffusion and intraparticle diffusion.

3.2.2. Isotherm

The isothermal experiments on the adsorption properties of B5, PB5, and KB5 on CIP are depicted in Fig. 2 f. The Langmuir model describes monomolecular layer adsorption on surfaces with a finite number of similar sites [49]. The Freundlich model mainly simulated non-uniform amorphous rows adsorption on adsorbent surfaces [50]. Langmuir and Freundlich were made to fit the experimental data, and the parameters of these models are shown in Table S2. The Langmuir model showed that the maximum adsorption capacity (Q_m) followed: PB5 (25.6 mg/g) > KB5 (8.77 mg/g) > B5 (3.71 mg/g). Temkin isotherm analysis (Table S2) further validated the role of chemical bonding, with binding energies (B = 18.2–24.5 J/mol) indicating strong adsorbate-adsorbent interaction [50]. The Freundlich adsorption isotherm was in very good conformity with the experiments, indicating that the CIP adsorption process on the three biochar samples was non-homogeneous [51].

The K_F values obtained from the Freundlich model have been reported to better reflect the affinity of biochar for the target pollutants [52]. K_F was also the adsorption coefficient, which represented the number of antibiotic molecules adsorbed by biochar per unit of equilibrium concentration [53]. Our fitting results showed that the K_F value: PB5 (26.11) > KB5 (5.38) > B5 (2.92), demonstrating H_3PO_4-modified biochar's superior CIP affinity which indicated that PB5 had the strongest affinity for CIP. These isotherm results corroborated kinetic data, confirming H_3PO_4 modification significantly enhances CIP adsorption.

3.3. Analysis of adsorption active site

To elucidate the underlying mechanisms, the surface functional groups contents of PB5, KB5, and B5 were further quantified using XPS. The C 1 s spectra of the biochar (Fig. S3) showed three peaks at approximately 284.8 eV (C—C), 285.3 eV (C—O), and 288.6 eV (C-COOH) [54,55]. Notably, H_3PO_4 modification did not significantly alter the C—C content on the biochar surface, but substantially increased the oxygen-containing functional groups: C—O increased from 25.4 % to 31.0 %, while C-COOH rose from 11.4 % to 17.7 %. In contrast, KOH treatment significantly enhanced the C—C content from 50.2 % to 61.7 %, without causing notable changes in C—O or C-COOH groups. These findings demonstrate that H_3PO_4 primarily modulates oxygenated functional groups, whereas KOH predominantly modifies the carbon structure.

Furthermore, we established a correlation between the relative contents of C—C, C—O, and C-COOH with Q_m/SSA (Fig. 3b). The positive correlation of both C—O and C-COOH with Q_m/SSA suggests that these surface functional groups serve as primary adsorption sites for CIP. To gain deeper mechanistic insights, we performed density functional theory (DFT) calculations to examine interactions between CIP and various functional groups. The adsorption energies were calculated for four representative structural units: C—H, C-OH, C═O, and C-COOH. As shown in Fig. 3c, carbon structures containing C-COOH groups exhibited the highest adsorption energy for CIP, while those with C—H, C-OH, or C═O groups showed relatively lower and similar adsorption energies. This result confirms that C-COOH groups are the predominant adsorption sites, with biochar containing more C-COOH groups demonstrating enhanced CIP adsorption capacity.

Additional analysis of interaction forces (Fig. 3d) revealed strong van der Waals interactions between CIP and the biochar matrix. Significantly, we observed hydrogen bond formation between the carboxyl groups (-COOH) and nitrogen atoms in CIP, generating additional electrostatic attraction. This dual interaction mechanism (van der Waals forces plus hydrogen bonding) accounts for the strong adsorption binding energy between C-COOH and CIP.

3.4. pH and anions effects on adsorption

Studies of adsorption-influencing factors help to explain experimental phenomena and understand the mechanism of adsorption. The adsorption behavior of ionizable organic compounds exhibits pH dependence correlating strongly with the compounds pK_a value [56]. The pK_a value demarcates pH ranges where different molecular species (cationic, neutral, or anionic form) predominatte.

As illustrated in Fig. 4a-c, we investigated the amount of CIP adsorbed on the solid phases of B5, PB5, and KB5 after 1 h and 18 h of reaction at different pH conditions. When increasing pH from 3, enhanced CIP adsorption occurred with B5 and KB5, attributable to the

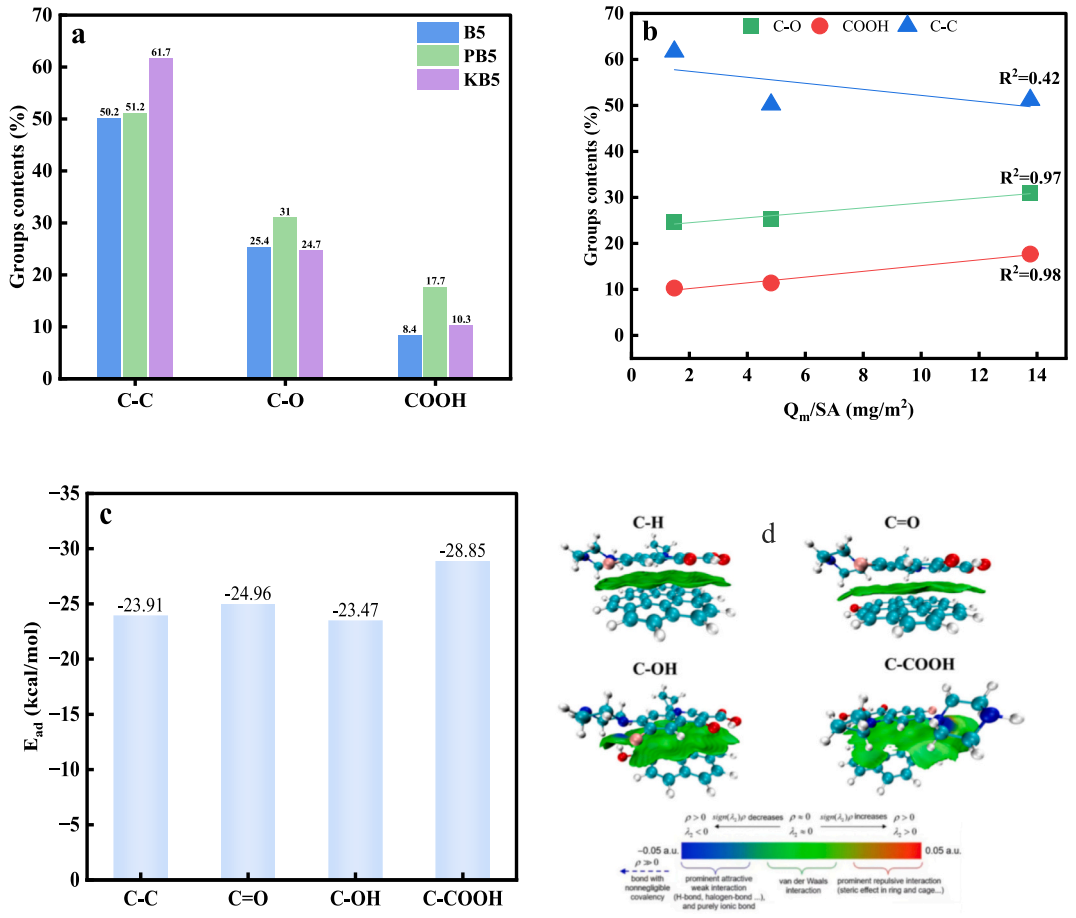

Fig. 3. (a) The functional groups contents of B5, PB5, and KB5 using XPS; (b) The relationship of functional groups contents and Q_m/SSA; (c) The adsorption energy between four functional groups and CIP; (d) The forces between CIP and C—H, C-OH, C-C=O, and C-COOH.

positively charged biochar surfaces at this pH (confirmed by zeta potential measurements in Fig. S4) that strengthened electrostatic attraction. Under alkaline conditions (pH 9) CIP adsorption by PB5 and KB5 was inhibited. The positive potential of H_3PO_4 and KOH-treated biochar was decreased, while the negative potential was significantly increased. The pKa of CIP was 8.7 [57]. When pH < 8.7, CIP was positively protonated, and when pH > 8.7, the presence of CIP species was negatively charged, and electrostatic interaction would suppress the CIP migration to the biochar surface. Notably, pristine biochar B5 showed no adsorption inhibition at initial pH 9, likely because KOH addition during pH adjustment increased its SSA, pore volume, and pore size. Furthermore, we observed suppressed CIP adsorption by PB5 at pH 3. Considering H_2SO_4 was used to regulate pH = 3, we hypothesized that the SO_4^{2-} anions might have a negative effect on the adsorption.

To test this hypothesis, we evaluated five anions (Cl^-, NO_3^-, HCO_3^-, CO_3^{2-}, and SO_4^{2-}) for their adsorption impacts (Fig. 4d-f). The results showed that monovalent anions had little effect on CIP adsorption, while divalent anions inhibited CIP adsorption to a greater extent. In the B5 and KB5 systems, the presence of HCO_3^- on the contrary led to an increase in the absorption of CIP, indicating that HCO_3^- had a certain promotion effect on CIP adsorption; the presence of CO_3^{2-} and SO_4^{2-} had a greater inhibition effect on the absorption of antibiotics, of which the inhibition effect of SO_4^{2-} reached 2.9 mg/g in the PB5 system. This phenomenon can be rationalized by: (i) pore structure densification, (ii) pore blocking, and (iii) particle aggregation induced by divalent anions [58,59], collectively reducing available binding sites. The pronounced inhibition in PB5 systems reflects its greater vulnerability due to larger pore size.

3.5. Mechanism of adsorption

CIP adsorption by biochar involves multiple mechanisms (Fig. 5). Firstly, physical adsorption plays a significant role. Biochar's extensive SSA and pore structure offer sites for CIP molecules. Unmodified biochar and those modified with acid or alkali possess enhanced surface areas and mesoporous structures. CIP molecules can attach to the surface via van der Waals forces and fill the pores. Secondly, chemical adsorption is crucial. H_3PO_4-modified PB5 contains enriched acidic functional groups (e.g., C-COOH). XPS analysis shows significant rises in C—O and C-COOH contents after H_3PO_4 modification. DFT calculations verified that carbon structures with C-COOH have the highest adsorption energy for CIP. The C-COOH forms hydrogen bonds and electrostatic forces with CIP, along with van der Waals forces, leading to strong adsorption. Alkaline-modified KB5 changes the carbon structure, also affecting adsorption. Chemical bonding between biochar's functional groups and CIP is the rate-limiting step, as described by the PSO model.

Electrostatic interaction further modulate adsorption. Solution PH influences biochar's surface charge. At acidic pH, biochar is positively charged, enhancing electrostatic attraction with CIP. At alkaline pH, the opposite occurs, inhibiting adsorption. Different ions also matter. Monovalent anions have a minor effect, while divalent anions, especially SO_4^{2-}, can inhibit CIP adsorption. In the PB5 system with a larger pore size, SO_4^{2-} has a more pronounced inhibitory effect due to pore structure changes and reduced adsorption sites. Overall, CIP adsorption on biochar is a combined result of surface area, pore structure, functional groups, and electrostatic interactions.

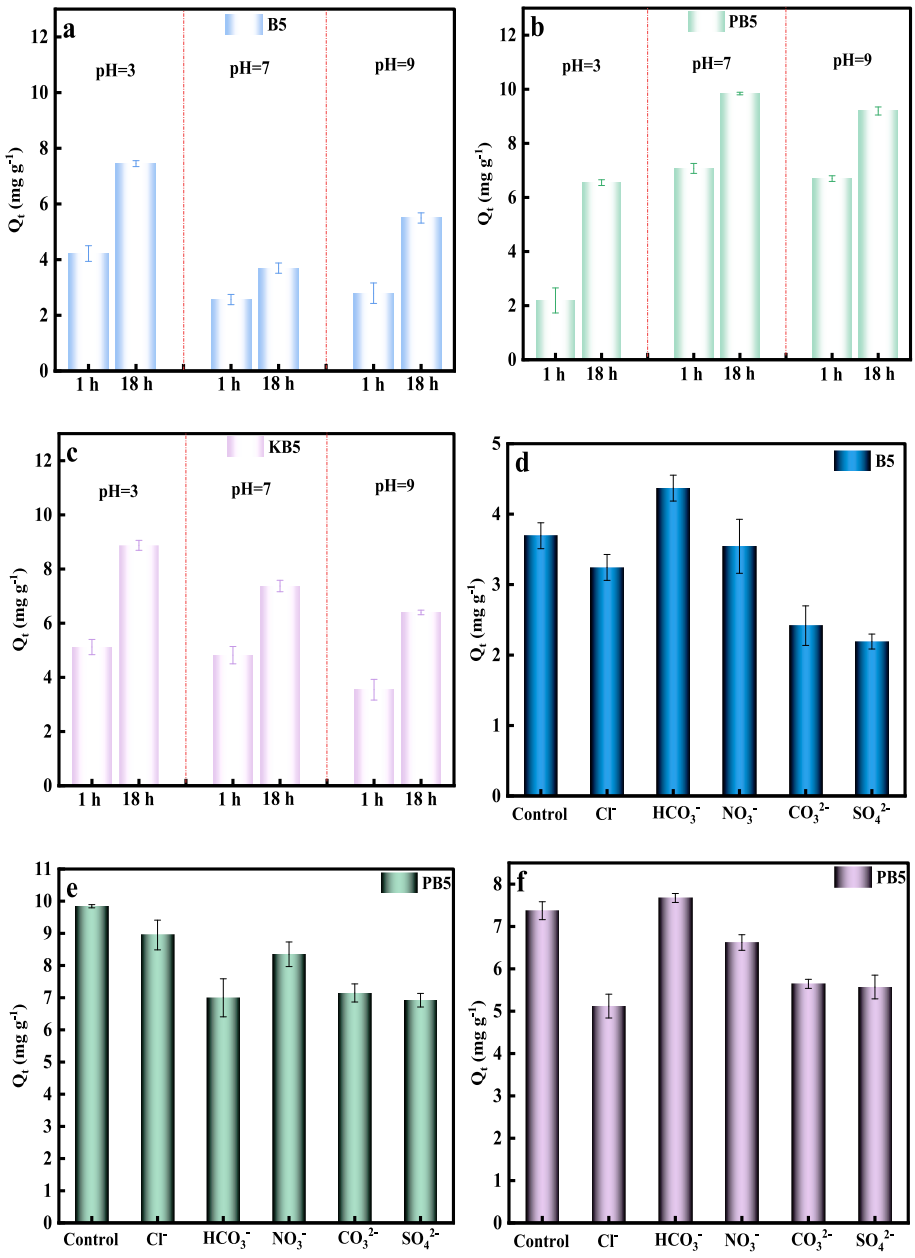

Fig. 4. (a, b, and c) The amount of CIP adsorbed on the solid phases of B5, PB5, and KB5 after 1 h and 18 h of reaction at different pH conditions; (d, e, and f) The effect of anions on CIP adsorption in the biochar reaction system.

4. Conclusions

In this study, PB5 and KB5 were prepared to investigate the effect of modification on antibiotic adsorption by biochar. Using CIP as a model contaminant, it was demonstrated that Acid-modified biochar (PB5) enhanced -COOH content (17.7 %) and pore size (131 Å), achieving 25.6 mg/g CIP adsorption. Alkali modification (KB5) prioritized specific surface area (5.92 m^2/g) but showed lower capacity (8.77 mg/g). Additionally, DFT confirmed -COOH as the primary active site, driving dual-force adsorption. Divalent anions ($SO4^{2-}$) inhibited adsorption more in PB5 due to pore blockage. In this regard, it is necessary to select more antibiotic model compounds, prepare and design different modified biochar, and systematically investigate the specific adsorption mechanism between the carbon structure of biochar and antibiotics in the future. Meanwhile, the establishment of a clear adsorption structure-activity relationship between biochar and antibiotics by combining efficient research tools such as machine learning can provide effective help to face the complex applications in the real environment.

Author contribution

All authors contributed to the study conception and design. The first draft of the manuscript was written by [Hui Wang] and all authors commented on previous versions of the manuscript. All authors read and approved the final manuscript.

Funding

This work was supported by Shanghai Municipal Education Commisson Project for Teachers' Professional Development.

CRediT authorship contribution statement

Hui Wang: Writing – original draft, Methodology. **Haoliang Wang:**

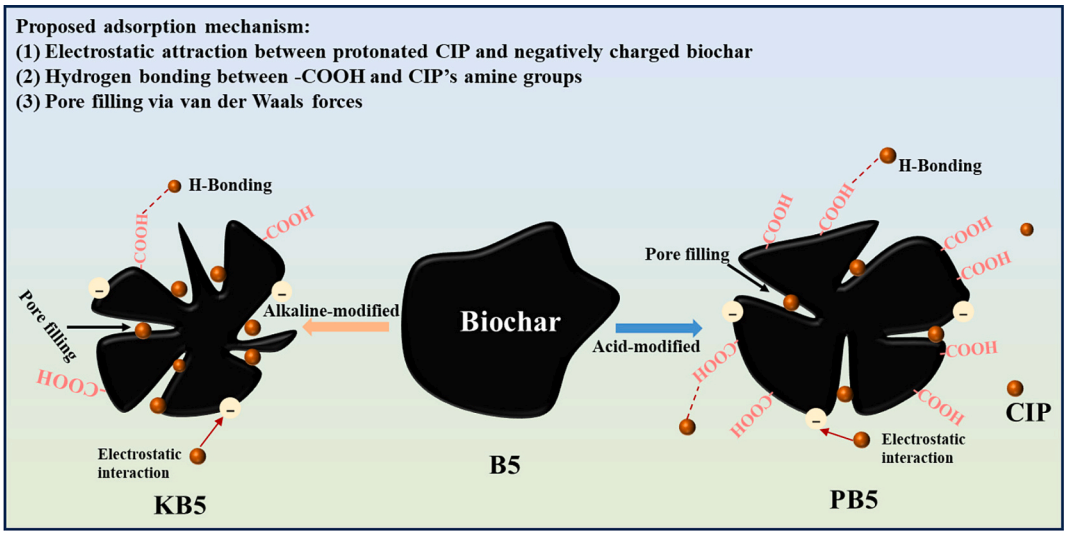

Fig. 5. Proposed adsorption mechanism of CIP via biochar samples.

Conceptualization. **Siyamak Shahab:** Writing – review & editing. **Hezhang Cheng:** Data curation. **Mikhail Atroshko:** Software. **Xianpeng Wang:** Software. **Meng Ye:** Resources.

Declaration of competing interest

The authors declare the following financial interests/personal relationships which may be considered as potential competing interests: Has patent pending to. If there are other authors, they declare that they have no known competing financial interests or personal relationships that could have appeared to influence the work reported in this paper.

Appendix A. Supplementary data

Supplementary data to this article can be found online at https://doi.org/10.1016/j.rechem.2025.102603.

Data availability

Data will be made available on request.

References

[1] H.Q. Anh, T.P.Q. Le, N. Da Le, X.X. Lu, T.T. Duong, J. Garnier, E. Rochelle-Newall, S.R. Zhang, N.H. Oh, C. Oeurng, et al., Antibiotics in surface water of east and southeast Asian countries: a focused review on contamination status, pollution sources, potential risks, and future perspectives, Sci. Total Environ. 764 (2021), https://doi.org/10.1016/j.scitotenv.2020.142865.

[2] X. Liu, J.C. Steele, X.Z. Meng, Usage, residue, and human health risk of antibiotics in Chinese aquaculture: a review, Environ. Pollut. 223 (2017) 161–169, https://doi.org/10.1016/j.envpol.2017.01.003.

[3] A.K. Sarmah, M.T. Meyer, A.B.A. Boxall, A global perspective on the use, sales, exposure pathways, occurrence, fate and effects of veterinary antibiotics (VAs) in the environment, Chemosphere 65 (2006) 725–759, https://doi.org/10.1016/j.chemosphere.2006.03.026.

[4] Y.G. Zhu, T.A. Johnson, J.Q. Su, M. Qiao, G.X. Guo, R.D. Stedtfeld, S.A. Hashsham, J.M. Tiedje, Diverse and abundant antibiotic resistance genes in Chinese swine farms, Proc. Natl. Acad. Sci. USA 110 (2013) 3435–3440, https://doi.org/10.1073/pnas.1222743110.

[5] X.P. Li, C.B. Wang, J.N. Tian, J.P. Liu, G.Y. Chen, Comparison of adsorption properties for cadmium removal from aqueous solution by biochar modified with different chemical reagents, Environ. Res. 186 (2020), https://doi.org/10.1016/j.envres.2020.109502.

[6] H.X. Mao, S.K. Wang, J.Y. Lin, Z.S. Wang, J. Ren, Modification of a magnetic carbon composite for ciprofloxacin adsorption, J. Environ. Sci. 49 (2016) 179–188, https://doi.org/10.1016/j.jes.2016.05.048.

[7] A.S. Oberoi, Y.Y. Jia, H.Q. Zhang, S.K. Khanal, H. Lu, Insights into the fate and removal of antibiotics in engineered biological treatment systems: a critical review, Environ. Sci. Technol. 53 (2019) 7234–7264. https://pubs.acs.org/doi/abs/10.1021/acs.est.9b01131.

[8] C. Yu, H. Pang, J.H. Wang, Z.Y. Chi, Q. Zhang, F.T. Kong, Y.P. Xu, S.Y. Li, J. Che, Occurrence of antibiotics in waters, removal by microalgae-based systems, and their toxicological effects: a review, Sci. Total Environ. 813 (2022), https://doi.org/10.1016/j.scitotenv.2021.151891.

[9] Z.Q. Wang, C.Y. Du, S.W. Lei, D.H. Ding, R.Z. Chen, S.J. Yang, T.M. Cai, Modulation of carbon induced persulfate activation by nitrogen dopants: recent advances and perspectives, J Mater Chem A 9 (2021) 25796–25826, https://doi.org/10.1039/D1TA08335J.

[10] H.Y. Zhao, Z.Q. Wang, Y.H. Liang, T.X. Wu, Y.L. Chen, J.R. Yan, Y.R. Zhu, D. H. Ding, Adsorptive decontamination of antibiotics from livestock wastewater by using alkaline-modified biochar, Environ. Res. 226 (2023), https://doi.org/10.1016/j.envres.2023.115676.

[11] B.W. Chen, Y. Yang, X.M. Liang, K. Yu, T. Zhang, X.D. Li, Metagenomic profiles of antibiotic resistance genes (ARGs) between human impacted estuary and Deep Ocean sediments, Environ. Sci. Technol. 47 (2013) 12753–12760, https://doi.org/10.1021/es403818e.

[12] H.Y. Chen, X.K. Li, L.W. Meng, G.G. Liu, X.C. Ma, C.Y. Piao, K. Wang, The fate and behavior mechanism of antibiotic resistance genes and microbial communities in anaerobic reactors treating oxytetracycline manufacturing wastewater, J. Hazard. Mater. 424 (2022), https://doi.org/10.1016/j.jhazmat.2021.127352.

[13] S.M. Zainab, M. Junaid, N. Xu, R.N. Malik, Antibiotics and antibiotic resistant genes (ARGs) in groundwater: a global review on dissemination, sources, interactions, environmental and human health risks, Water Res. 187 (2020), https://doi.org/10.1016/j.watres.2020.116455.

[14] S.K. Bhatia, A.K. Palai, A. Kumar, R.K. Bhatia, A.K. Patel, V.K. Thakur, Y.K. Yang, Trends in renewable energy production employing biomass-based biochar, Bioresour. Technol. 340 (2021), https://doi.org/10.1016/j.biortech.2021.125644.

[15] A.C. Sophia, E.C. Lima, Removal of emerging contaminants from the environment by adsorption, Ecotoxicol. Environ. Saf. 150 (2018) 1–17, https://doi.org/10.1016/j.ecoenv.2017.12.026.

[16] Y.D. Chen, Y.C. Lin, S.H. Ho, Y. Zhou, N.Q. Ren, Highly efficient adsorption of dyes by biochar derived from pigments-extracted macroalgae pyrolyzed at different temperature, Bioresour. Technol. 259 (2018) 104–110, https://doi.org/10.1016/j.biortech.2018.02.094.

[17] J. Fang, L. Jin, Q.K. Meng, S.D. Shan, D.J. Wang, D.H. Lin, Biochar effectively inhibits the horizontal transfer of antibiotic resistance genes via transformation, J. Hazard. Mater. 423 (2022), https://doi.org/10.1016/j.jhazmat.2021.127150.

[18] Y.C. Zhou, S.Y. Leong, Q.L. Li, Modified biochar for removal of antibiotics and antibiotic resistance genes in the aqueous environment: a review, J Water Process Eng 55 (2023), https://doi.org/10.1016/j.jwpe.2023.104222.

[19] L. Jia, P. Cheng, Y. Yu, S.H. Chen, C.X. Wang, L. He, H.T. Nie, J.C. Wang, J. C. Zhang, B.G. Fan, et al., Regeneration mechanism of a novel high-performance biochar mercury adsorbent directionally modified by multimetal multilayer loading, J. Environ. Manag. 326 (2023), https://doi.org/10.1016/j.jenvman.2022.116790.

[20] C.Y. Li, X.X. Zhu, H.L. He, Y.X. Fang, H.P. Dong, J.H. Lü, J.F. Li, Y.M. Li, Adsorption of two antibiotics on biochar prepared in air-containing atmosphere: influence of biochar porosity and molecular size of antibiotics, J. Mol. Liq. 274 (2019) 353–361, https://doi.org/10.1016/j.molliq.2018.10.142.

[21] X.B. Zhang, Y.C. Zhang, H.H. Ngo, W.S. Guo, H.T. Wen, D. Zhang, C.C. Li, L. Qi, Characterization and sulfonamide antibiotics adsorption capacity of spent coffee grounds based biochar and hydrochar, Sci. Total Environ. 716 (2020), https://doi.org/10.1016/j.scitotenv.2020.137015.

[22] H. Huang, J.C. Tang, K. Gao, R.Z. He, H. Zhao, D. Werner, Characterization of KOH modified biochars from different pyrolysis temperatures and enhanced adsorption of antibiotics, RSC Adv. 7 (2017) 14640–14648, https://doi.org/10.1039/C6RA27881G.

[23] Q.B. Shen, Z.Y. Wang, Q. Yu, Y. Cheng, Z.D. Liu, T.P. Zhang, S.Q. Zhou, Removal of tetracycline from an aqueous solution using manganese dioxide modified biochar derived from Chinese herbal medicine residues, Environ. Res. 183 (2020), https://doi.org/10.1016/j.envres.2020.109195.
[24] J. Zhao, G.W. Liang, X.L. Zhang, X.W. Cai, R.N. Li, X.Y. Xie, Z.W. Wang, Coating magnetic biochar with humic acid for high efficient removal of fluoroquinolone antibiotics in water, Sci. Total Environ. 688 (2019) 1205–1215, https://doi.org/10.1016/j.scitotenv.2019.06.287.
[25] X.L. Hu, Y.W. Xue, L. Long, K.J. Zhang, Characteristics and batch experiments of acid- and alkali-modified corncob biomass for nitrate removal from aqueous solution, Environ. Sci. Pollut. R. 25 (2018) 19932–19940, https://doi.org/10.1007/s11356-018-2198-5.
[26] B.N. Jiang, Y.Q. Lin, J.C. Mbog, Biochar derived from swine manure digestate and applied on the removals of heavy metals and antibiotics, Bioresour. Technol. 270 (2018) 603–611, https://doi.org/10.1016/j.biortech.2018.08.022.
[27] X. Zhang, D.D. Gang, J.J. Zhang, X.B. Lei, Q.Y. Lian, W.E. Holmes, M.E. Zappi, H. Yao, Insight into the activation mechanisms of biochar by boric acid and its application for the removal of sulfamethoxazole, J. Hazard. Mater. 424 (2022), https://doi.org/10.1016/j.jhazmat.2021.127333.
[28] A. Gupta, A. Garg, Adsorption and oxidation of ciprofloxacin in a fixed bed column using activated sludge derived activated carbon, J. Environ. Manag. 250 (2019), https://doi.org/10.1016/j.jenvman.2019.109474.
[29] T.B. Nguyen, Q.M. Truong, C.W. Chen, W.H. Chen, C.D. Dong, Pyrolysis of marine algae for biochar production for adsorption of ciprofloxacin from aqueous solutions, Bioresour. Technol. 351 (2022), https://doi.org/10.1016/j.biortech.2022.127043.
[30] S. Lagergren, Zur Theorie der Sogenannten Adsorption Gelöster Stoffe, Kungliga Svenska Vetenskapsakademiens. Handlingar 24 (1898) 1–39, https://doi.org/10.1007/BF01501332.
[31] Y.-S. Ho, Second-order kinetic model for the sorption of cadmium onto tree fern: a comparison of linear and non-linear methods, Water Res. 40 (2006) 119–125, https://doi.org/10.1016/j.watres.2005.10.040.
[32] J. Weber, J.C. Morris, Weber W kinetics of adsorption of carbon from solution, J. Sanit. Eng. Div. Am. Soc. Civil Eng. (1963) 36–60.
[33] I. Langmuir, The adsorption of gases on plane surfaces of glass, mica and platium, J. Am. Chem. Soc. 40 (1918) 1361–1403, https://doi.org/10.1021/ja02242a004.
[34] H. Freundlich, Über die Adsorption in Lösungen, Z. Phys. Chem. 57 (1906) 385–470.
[35] S.N. Jain, P.R. Gogate, Efficient removal of acid green 25 dye from wastewater using activated as biosorbent: batch and column studies, J. Environ. Manag. 210 (2018) 226–238, https://doi.org/10.1016/j.jenvman.2018.01.008.
[36] T. Lu, F.W. Chen, Multiwfn: a multifunctional wavefunction analyzer, J. Comput. Chem. 33 (2012) 580–592, https://doi.org/10.1002/jcc.22885.
[37] H.A. Almodarresiyeh, S.N. Shahab, V.M. Zelenkovsky, V.E. Agabekov, Electronic structure and absorption spectra of sodium 2-hydroxy-5-({2-methoxy-4 [(4-sulfophenyl) diazenyl] phenyl} diazenyl) benzoate, J. Appl. Spectrosc. 81 (2014) 161–163, https://doi.org/10.1007/s10812-014-9903-z.
[38] A.U. Rajapaksha, Y.S. Ok, A. El-Naggar, H. Kim, F.H. Song, S. Kang, Y.F. Tsang, Dissolved organic matter characterization of biochars produced from different feedstock materials, J. Environ. Manag. 233 (2019) 93–99, https://doi.org/10.1016/j.jenvman.2018.12.069.
[39] N. Soltani, A. Bahrami, M.I. Pech-Canul, L.A. González, Review on the physicochemical treatments of rice husk for production of advanced materials, Chem. Eng. J. 264 (2015) 899–935, https://doi.org/10.1016/j.cej.2014.11.056.
[40] Z.H. Zhang, L.F. Cui, Y. Zhang, L.H. Klausen, M.Y. Chen, D. Sun, S.Y. Xu, S.F. Kang, J.Y. Shi, Regulation of carboxyl groups and structural defects of graphitic carbon nitride via environmental-friendly glucose oxidase ring-opening modulation, Appl. Catal. B Environ. 297 (2021), https://doi.org/10.1016/j.apcatb.2021.120441.
[41] J.F. Yu, L. Tang, Y. Pang, G.M. Zeng, J.J. Wang, Y.C. Deng, Y.N. Liu, H.P. Feng, S. Chen, X.Y. Ren, Magnetic nitrogen-doped sludge-derived biochar catalysts for persulfate activation: internal electron transfer mechanism, Chem. Eng. J. 364 (2019) 146–159, https://doi.org/10.1016/j.cej.2019.01.163.
[42] T.T. Qin, M.K. Song, K.K. Jiang, J.W. Zhou, W. Zhuang, Y. Chen, D. Liu, X.C. Chen, H.J. Ying, J.L. Wu, Efficient decolorization of citric acid fermentation broth using carbon materials prepared from phosphoric acid activation of hydrothermally treated corncob, RSC Adv. 7 (2017) 37112–37121, https://doi.org/10.1039/C7RA04813K.
[43] W. Hu, Y.L. Niu, T.M. Shen, K. Dong, D.Q. Wang, Magnetic biochar prepared by a dry process for the removal of sulfonamides antibiotics from aqueous solution, J. Mol. Liq. 400 (2024), https://doi.org/10.1016/j.molliq.2024.124576.
[44] J. Liu, H.H. Liu, X.Y. Yang, X.P. Jia, M.F. Cai, Y.C. Bao, Preparation of Si-Mn/biochar composite and discussions about characterizations, advances in application and adsorption mechanisms, Chemosphere 281 (2021), https://doi.org/10.1016/j.chemosphere.2021.130946.
[45] X.Y. Xu, Y.C. Weng, J.L. Zhuang, H.F. Pei, B.D. Wu, W. Wu, J.J. Yang, B. Wang, T. Y. Huang, Enhanced adsorption capacity of antibiotics by calamus-biochar with phosphoric acid modification: performance assessment and mechanism analysis, J. Taiwan Inst. Chem. Eng. 161 (2024), https://doi.org/10.1016/j.jtice.2024.105541.
[46] Y.J. Yuan, Q. Wu, W.B. Cao, S.Y. Fang, J.S. Cao, W.J. Liu, J.Y. Luo, Recycling crayfish shell and waste activated sludge as biochar to in-situ enhance antibiotics removal from wastewater: linking structure properties and reaction kinetics, J Water Process Eng 63 (2024), https://doi.org/10.1016/j.jwpe.2024.105517.
[47] O.A. Ajala, S.O. Akinnawo, A. Bamisaye, D.T. Adedipe, M.O. Adesina, O.A. Okon-Akan, T.A. Adebusuyi, A.T. Ojedokun, K.A. Adegoke, O.S. Bello, Adsorptive removal of antibiotic pollutants from wastewater using biomass/biochar-based adsorbents, RSC Adv. 13 (2023) 4678–4712, https://doi.org/10.1039/D2RA06436G.
[48] Y.F. Ma, T.M. Lu, L. Yang, L. Wu, P. Li, J.Y. Tang, Y.L. Chen, F. Gao, S. Cui, X.B. Qi, et al., Efficient adsorptive removal of fluoroquinolone antibiotics from water by alkali and bimetallic salts co-hydrothermally modified sludge biochar, Environ. Pollut. 298 (2022), https://doi.org/10.1016/j.envpol.2022.118833.
[49] S. Afshin, Y. Rashtbari, M. Vosough, A. Dargahi, M. Fazlzadeh, A. Behzad, M. Yousefi, Application of box-Behnken design for optimizing parameters of hexavalent chromium removal from aqueous solutions using Fe3O4 loaded on activated carbon prepared from alga: kinetics and equilibrium study, J Water Process Eng 42 (2021), https://doi.org/10.1016/j.jwpe.2021.102113.
[50] M.V. Niri, A.H. Mahvi, M. Alimohammadi, M. Shirmardi, H. Golastanifar, M. J. Mohammadi, et al., Removal of natural organic matter (NOM) from an aqueous solution by NaCl and surfactant-modified clinoptilolite, J. Water Health 13 (2015) 394–405, https://doi.org/10.2166/wh.2014.088.
[51] S. Cai, Q. Zhang, Z.Q. Wang, S. Hua, D.H. Ding, T.M. Cai, R.H. Zhang, Pyrrolic N-rich biochar without exogenous nitrogen doping as a functional material for bisphenol a removal: performance and mechanism, Appl. Catal. B Environ. 291 (2021), https://doi.org/10.1016/j.apcatb.2021.120093.
[52] S.D. Wang, L.J. Kong, J.Y. Long, M.H. Su, Z.H. Diao, X.Y. Chang, D.Y. Chen, G. Song, K. Shih, Adsorption of phosphorus by calcium-flour biochar: isotherm, kinetic and transformation studies, Chemosphere 195 (2018) 666–672, https://doi.org/10.1016/j.chemosphere.2017.12.101.
[53] L.K. Lazzari, V.B. Zampieri, R.M. Neves, M. Zanini, A.J. Zattera, C. Baldasso, A study on adsorption isotherm and kinetics of petroleum by cellulose cryogels, Cellulose 26 (2019) 1231–1246. https://link.springer.com/article/10.1007/s10570-018-2111-x.
[54] H. Wang, H. Wang, S. Shahab, et al., Charge-transfer interactions between antibiotics and small organic acids: spectroscopic characterization and computational investigation, J. Mol. Struct. 1322 (2025), https://doi.org/10.1016/j.molstruc.2024.140580.
[55] S. Shahab, M. Sheikhi, L. Filippovich, et al., Synthesis, geometry optimization, spectroscopic investigations (UV/Vis, excited states, FT-IR) and application of new azomethine dyes, J. Mol. Struct. 1148 (2017), https://doi.org/10.1016/j.molstruc.2017.07.036.
[56] H.B. Li, D. Zhang, X.Z. Han, B.S. Xing, Adsorption of antibiotic ciprofloxacin on carbon nanotubes: pH dependence and thermodynamics, Chemosphere 95 (2014) 150–155, https://doi.org/10.1016/j.chemosphere.2013.08.053.
[57] T.K.T. Nguyen, T.B. Nguyen, W.H. Chen, C.W. Chen, A.K. Patel, X.T. Bui, L.J. Chen, R.R. Singhania, C.D. Dong, Phosphoric acid-activated biochar derived from sunflower seed husk: selective antibiotic adsorption behavior and mechanism, Bioresour. Technol. 371 (2023), https://doi.org/10.1016/j.biortech.2023.128593.
[58] X.Y. Zeng, Y. Wang, R.X. Li, H.L. Cao, Y.F. Li, J. Lu, Impacts of temperatures and phosphoric-acid modification to the physicochemical properties of biochar for excellent sulfadiazine adsorption, Biochar 4 (2022), https://doi.org/10.1007/s42773-022-00143-4.
[59] C. Peiris, S. Nawalage, J.J. Wewalwela, S.R. Gunatilake, M. Vithanage, Biochar based sorptive remediation of steroidal estrogen contaminated aqueous systems: a critical review, Environ. Res. 191 (2020), https://doi.org/10.1016/j.envres.2020.110183.